On Grasp Quality Measures: Grasp Robustness and Contact Force Distribution in Underactuated and Compliant Robotic Hands

On Grasp Quality Measures: Grasp Robustness and Contact Force Distribution in Underactuated and Compliant Robotic Hands

Maria Pozzi, Monica Malvezzi, and Domenico Prattichizzo

***Abstract*—The availability of grasp quality measures is fundamental for grasp planning and control, and also to drive designers in the definition and optimization of robotic hands. This work investigates on grasp robustness and quality indexes that can be applied to power grasps with underactuated and compliant hands. When dealing with such types of hands, there is the need of an evaluation method that takes into account the forces that can be actually controlled by the hand, depending on its actuation system. In this paper, we study the potential contact robustness and the potential grasp robustness (PCR, PGR) indexes. They both consider main grasp properties: contact points, friction coefficient, etc., but also hand degrees of freedom and consequently, the directions of controllable contact forces. The PCR comes directly from the classical grasp theory and can be easily evaluated, but often leads to too conservative solutions, particularly when the grasp has many contacts. The PGR is more complex and computationally heavier, but gives a more realistic, even if still conservative, estimation of the overall grasp robustness, also in power grasps. We evaluated the indexes for various simulated grasps, performed with underactuated and compliant hands, and we analyzed their variations with respect to the main grasp parameters.**

***Index Terms*—Grasping, multifingered hands.**

I. Introduction

QUANTIFYING the quality of a grasp performed by a robotic hand or, more in general, by a robotic system that can manipulate objects (e.g. teams of cooperating robots, humanoids, etc.), plays a key role in several aspects of a manipulation task. During the planning phase, a grasp quality measure is necessary to find the optimal position of the hand with respect to the object to be grasped, and adjust the contact forces. While executing a manipulation sequence, local optimization with respect to grasp performances indexes can be used to react to external disturbances.

Manuscript received June 5, 2016; revised August 12, 2016; accepted September 5, 2016. Date of publication September 21, 2016; date of current version October 6, 2016. This paper was recommended for publication by Associate Editor H. Liu and Editor H. Ding upon evaluation of the reviewers' comments. This work was supported by the European Union's Horizon 2020 Research and Innovation Programme under Grant 688857 of the project Soft-Pro: "Synergy-based Open-source Foundations and Technologies for Prosthetics and RehabilitatiOn," and under Grant 645599 of the project SoMa: "Soft-bodied intelligence for Manipulation."

The authors are with the Department of Information Engineering and Mathematics, University of Siena, Siena 53100, Italy, and also with the Department of Advanced Robotics, Istituto Italiano di Tecnologia, Genoa 16163, Italy (e-mail: pozzi@diism.unisi.it; malvezzi@diism.unisi.it; prattichizzo@diism.unisi.it).

Color versions of one or more of the figures in this letter are available online at http://ieeexplore.ieee.org.

Digital Object Identifier 10.1109/LRA.2016.2612304

One desirable property of a grasp is disturbance resistance, that is achieved when the hand can prevent any movement of the object due to external wrenches. This can happen because the fingers envelop the object and constraint it geometrically (*form closure*) or because proper forces are exerted at the contacts (*force closure*) [1].

Grasp quality measures can also be employed to find the optimal design characteristics, e.g. number of fingers, type of actuation, overall dimension, etc., of a robotic hand. In [2], for instance, authors present a modular approach to robotic hands design that allows for finding a trade off between a simple gripper and a more complex anthropomorphic manipulator.

A recent trend in the design of robotic hands is to make them underactuated and compliant. Compliance allows the hands to be adaptable to different objects, whereas underactuation is a way to reduce the complexity of the hand. There are many ways in which underactuation can be achieved. A fixed mechanical motion coupling between hand joints, for example, is adopted to reduce the number of hand degrees of freedom (DoFs) in [3], while in [4] hand joints have passive compliance, that allows to keep adaptability properties and to gain robustness with respect to uncertainties. New robotic hands like the Pisa/IIT SoftHand+ [5] and the RBO Hand 2 [6], have underactuation and compliance as their main features and strengths.

In order to maintain the versatility properties while simplifying the robotic hand structure through underactuation and passive joints, theoretical tools that allow to design and optimize hand parameters are needed. Towards this objective, the form closure property has been extended to underactuated hands in [7], while in [8] dexterous manipulation properties with underactuated elastic hands are discussed. In [9] the author discusses the problem of force isotropy in underactuated hands, this characteristic guarantees a uniform distribution of forces over the grasped object and prevents object damages due to force unbalances. The above cited papers are mainly focused on the hand's structure and actuation system, and do not account for other grasping properties such as friction, and contact force limits. There are many quality measures that can account for these characteristics. One of the most largely used in the literature is the Largest Minimum Resisted Wrench, that was firstly introduced by Ferrari and Canny [10]. This measure computes the largest perturbation wrench that the grasp can resist in any direction, without considering hand compliance, actuation, and controllability. Thus, it is not guaranteed that the set of optimal forces evaluated with the Ferrari-Canny index can actually be applied by the hand to the object.

A comprehensive list and description of the grasp quality measures that have been proposed in the literature can be found in [11]. Most of the indexes analyzed by the authors are thought for fully-actuated hands and precision grasps, and either are based on the position of the contact points on the object surface, or take into account the configuration of the hand.

The aim of this paper is to define criteria to quantify grasp robustness and stability that can be applied to a wide set of grasps, including grasps with many contact points realized with compliant underactuated hands, taking into account the main grasp properties (contact force limits, friction, contact points, etc.).

Intuitively, the robustness of a grasp increases as the number of contacts increases, and its controllability is improved when a higher number of actuators is available. Furthermore, when the hand has a limited number of actuators, adaptability and grasp capabilities can be recovered by exploiting compliance. The objective of this paper is to define quantitative measures able to represent all these qualitative observations. Underactuated and compliant hands tend to perform many-contact (or power, enveloping) grasps to stably hold objects. In [12], Pollard proposes an algorithm for the synthesis of such type of grasps, but does not take into account hand characteristics. One of the problems in power grasp modeling is the definition of contact force distribution, since often the problem is statically indeterminate and the static equilibrium equations are not sufficient to define a unique solution. In [13] the authors propose a solution based on the evaluation of contact sliding compatible with rigid body motions.

In [14] Bicchi defined the subspace of controllable internal forces, namely the internal forces that can be modified by the hand according to its actuators. To solve the indeterminacy arising in hyperstatic or statically indeterminate grasps, he removed the rigid body kinematic assumption for the contacts between the hand and the object, and adopted a lumped linear elastic stiffness model. In [15] the definition of form closure and force closure are summarized, and a method to evaluate force closure properties taking into account the actually controllable internal forces, is proposed. This approach is based on the assumption of a linear elastic model for the tangential contact force, so the direction and magnitude of the contact force are constrained by the system kinematics. However, in a quasi-static framework, contact forces can assume arbitrary value and direction within the friction cone. This is why Prattichizzo *et al.* in [16] claim that the measure of force closure presented in [15], and called Potential Contact Robustness (PCR), is overconservative, and introduce the Potential Grasp Robustness (PGR), an index of force closure suitable power grasps. Despite it is a quite preliminary work, the paper proposes a solution to a problem that is becoming more and more important, due to the development of underactuated compliant hands. For this reason we decided to extend it and to evaluate whether the PGR can be a good quality measure for underactuated compliant hands.

Consider the grasp in Fig. 1, in which a robot (a finger or an arm) is grasping an object in four contact points. We assume that the robot is underactuated, i.e. the forces that the links can apply to the object through the contacts cannot be independently controlled. In particular, we suppose that the robot has only one actuator, and that the four joints are mutually connected to a tendon. Let us suppose that the object is subject to a wrench $\mathbf{g}_0$ and that the actuator applies a torque $\boldsymbol{\tau}_{0,1}$. According to the results on force controllability presented in [14] and extended to hands actuated by soft synergies in [17], in our example the dimension of the subspace of controllable internal forces is one, because there is only one actuator, and assuming a linearized model, the directions of the controllable internal forces and the ratio between their magnitudes are constant, since they can be defined with a one–dimensional parameter. Let us assume that such directions are those identified with the bold red arrows in the figure. Three of them are within the friction cone, while $\boldsymbol{\lambda}_{0,3}$ is very close to its boundary. If we compute the grasp quality according to the PCR measure, that evaluates the distance from the violation of the friction constraints considering all the contact points, we get a value close to zero, but actually the grasp is stable, since three of the four contacts are sufficient to guarantee its stability. This information can be captured by the PGR.

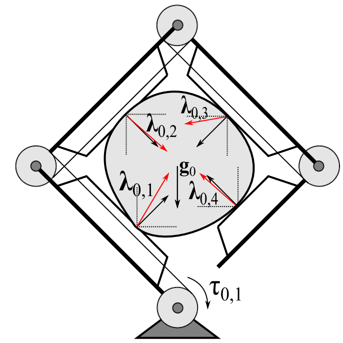

Fig. 1. Example of a single compliant underactuated robotic arm grasping an object through four contact points.

In this paper, after an overview of the main definitions and hypotheses related to the grasp model (Section II), we propose an efficient implementation of the PGR (Section III), and we investigate its applicability to power grasps and underactuated hands with numerical simulations (Section IV). Section V draws the conclusion of the work and its future developments.

II. Underactuated and Compliant Grasps

The notation and the main definitions introduced in [1] are adopted. Let us consider a hand grasping an object in a static equilibrium condition. Let us define $\{\mathbf{N}\}$ and $\{\mathbf{B}\}$ as the reference frames fixed in the workspace and on the object, respectively. Let $\mathbf{u} \in \mathbb{R}^6$ be a vector defining the position and orientation of $\{\mathbf{B}\}$ with respect to $\{\mathbf{N}\}$. The hand configuration is described by vector $\mathbf{q} \in \mathbb{R}^{n_q}$, where n_q is the number of hand joints. The grasped object is rigid and subject to an external wrench $\mathbf{g} \in \mathbb{R}^6$, while the joint actuators apply a series of torques that can be collected in the vector $\boldsymbol{\tau} \in \mathbb{R}^{n_q}$.

We make the widely accepted hypothesis that the contacts between the hand and the object are concentrated in a finite number n_c of contact points. Let us indicate with $\mathbf{c}_i$ the coordinates of the i-th, $i = 1, \cdots, n_c$ contact point on the object with respect to $\{\mathbf{N}\}$. At each contact point, we define a reference frame $\{\mathbf{C}\}_i$ with axes $\{\mathbf{n}_i, \mathbf{t}_i, \mathbf{o}_i\}$, expressed in $\{\mathbf{N}\}$. The unit vector $\mathbf{n}_i \in \mathbb{R}^3$ is normal to the contact surface at the contact point and points towards the object interior.

Different models can be adopted to describe contact forces, in this paper, for the sake of simplicity, we assume a Single Point with Friction (SPwF) contact model [1], [18], i.e. at each contact point the hand link applies to the object a generic force $\boldsymbol{\lambda}_i \in \mathbb{R}^3$, $i = 1, \cdots, n_c$. Let us collect all the contact forces in a vector $\boldsymbol{\lambda} \in \mathbb{R}^{n_\lambda}$; under the hypothesis of SPwF contact model, $n_\lambda = 3n_c$.

Grasp static equilibrium is described by the following equations

$$\mathbf{g} = -\mathbf{G}\boldsymbol{\lambda}, \qquad \boldsymbol{\tau} = \mathbf{J}^{\mathrm{T}}\boldsymbol{\lambda} \tag{1}$$

where $\mathbf{G} \in \mathbb{R}^{6 \times n_\lambda}$ is the Grasp matrix, while $\mathbf{J} \in \mathbb{R}^{n_\lambda \times n_q}$ is the hand Jacobian matrix [18].

When $\mathcal{N}(\mathbf{G}) \cap \mathcal{N}(\mathbf{J}^{\mathrm{T}}) \neq \mathbf{0}$, the algebraic system composed of the two equations in (1) does not admit a unique solution for the contact force $\boldsymbol{\lambda}$. The problem has been solved in [14] in a linearized quasistatic framework assuming that the violation of the kinematics contact constraint is related to contact force variation, through a model of contact stiffness. Let us therefore consider an initial equilibrium configuration and let us apply to it a *small* perturbation. We will indicate with the index $_0$ the variables in the initial configuration, and with Δ the variation of system variables with respect to the reference equilibrium. The simpler contact stiffness model is linear and can be expressed as

$$\Delta\boldsymbol{\lambda} = \mathbf{K}_c \left(\mathbf{J}\Delta\mathbf{q} - \mathbf{G}^T \Delta\mathbf{u}\right) \tag{2}$$

where $\mathbf{K}_c \in \mathbb{R}^{n_\lambda \times n_\lambda}$ is the contact stiffness matrix, symmetric and positive definite.

We can take the stiffness of the hand structure into account by relating joint action variations $\Delta\boldsymbol{\tau}$ to the difference between a reference value of joint parameters $\Delta\mathbf{q}_r$ and their actual value $\Delta\mathbf{q}$, i.e. $\Delta\boldsymbol{\tau} = \mathbf{K}_q(\Delta\mathbf{q}_r - \Delta\mathbf{q})$, where $\mathbf{K}_q \in \mathbb{R}^{n_q \times n_q}$ is the joint stiffness matrix, symmetric and positive definite. If the hand joints are coordinated according to a set of postural synergies, as discussed in [17], the reference values of joint parameters $\Delta\mathbf{q}_r$ can be evaluated as $\Delta\mathbf{q}_r = \mathbf{S}\Delta\mathbf{z}$, where $\mathbf{S} \in \mathbb{R}^{n_q \times n_z}$ is the synergy matrix, and $\mathbf{z} \in \mathbb{R}^{n_z}$ is the synergy input vector. In this work, for the sake of simplicity, we neglect the geometrical terms, i.e. the variations of $\mathbf{G}$ and $\mathbf{J}$ matrices. For a complete discussion of the quasistatic model including such terms, the reader can refer to [17].

The general solution of the system (1), considering a variation with respect to an initial equilibrium configuration, is $\Delta\boldsymbol{\lambda} = \mathbf{G}_{\mathbf{K}}^R \Delta\mathbf{g} + \Delta\boldsymbol{\lambda}_h + \Delta\boldsymbol{\lambda}_s$, where $\mathbf{G}_{\mathbf{K}}^R = \mathbf{K}\mathbf{G}^{\mathrm{T}}\left(\mathbf{G}\mathbf{K}\mathbf{G}^{\mathrm{T}}\right)^{-1}$ is the $\mathbf{K}$-weighted pseudoinverse of $\mathbf{G}$, $\Delta\boldsymbol{\lambda}_h$ represents the controllable internal forces, i.e. the internal forces that can be actively modified by hand actuators, and $\Delta\boldsymbol{\lambda}_s$ represents the internal structural forces. Stiffness matrix $\mathbf{K}$ takes into account both contact and joint stiffness and, neglecting geometrical effects, it can be evaluated as $\mathbf{K} = \left(\mathbf{K}_c^{-1} + \mathbf{J}\mathbf{K}_q^{-1}\mathbf{J}^{\mathrm{T}}\right)^{-1}$.

The complete solution of the problem and the analysis of controllable and structural internal forces have been investigated in [14], and extended to synergy actuated hands in [17]. In these papers authors showed that controllable internal forces belong to a subspace $\mathcal{F}_h$ expressed as in Eq. (3).

$$\mathcal{F}_h = \mathcal{R}(\mathbf{E}) = \mathcal{N}(\mathbf{G}) \cap \left(\mathcal{R}(\mathbf{KJS}) + \mathcal{R}(\mathbf{KG}^{\mathrm{T}})\right) \tag{3}$$

Matrix $\mathbf{E} \in \mathbb{R}^{n_\lambda \times h}$ defines a base of such subspace, so the controllable internal forces can be defined as $\Delta\boldsymbol{\lambda}_h = \mathbf{E}\boldsymbol{y}$, where $\mathbf{y} \in \mathbb{R}^h$ is a generic vector. The small perturbation applied to the initial reference equilibrium configuration produces a new distribution of contact forces that is given by $\boldsymbol{\lambda} = \boldsymbol{\lambda}_0 + \Delta\boldsymbol{\lambda}$. Let us consider the i-th contact point. The vector of the contact forces $\boldsymbol{\lambda}_i$ with normal component $\lambda_{i,n}$, and tangential components, $\lambda_{i,t}$ and $\lambda_{i,o}$, must satisfy the unilateral constraint in (4) and the Coulomb friction constraint in (5), so to avoid detachment and slippage of the contact.

$$\lambda_{i,n} \geq 0 \tag{4}$$

$$\sqrt{\lambda_{i,t}^2 + \lambda_{i,o}^2} \leq \mu_i \lambda_{i,n} \tag{5}$$

In Eq. (5), μ_i indicates the friction coefficient, that depends on surface materials.

III. Grasp Quality Indexes

A. *Definitions*

Given the notation and the equations summarized in Section II, let us define the vector $\mathbf{d}(\boldsymbol{\lambda}) = [d_{1,c}, d_{1,f}, d_{1,\max}, \ldots, d_{n_c,c}, d_{n_c,f}, d_{n_c,\max}]^{\mathrm{T}} \in \mathbb{R}^{3n_c}$, where $d_{i,c}$ is the contact force component normal to the contact surface, i.e. $d_{i,c} = \boldsymbol{\lambda}_i^{\mathrm{T}}\mathbf{n}_i$, $d_{i,f}$ is the distance of $\boldsymbol{\lambda}_i$ from the friction cone surface, and $d_{i,\max} = f_{i,\max} - \| \boldsymbol{\lambda}_i \|$, assuming that there is a maximum applicable force $f_{i,\max}$ at each contact. Let us call $d_{\min}^{\mathcal{F}_h}$ the minimum element of vector $\mathbf{d}(\boldsymbol{\lambda})$, computed considering only controllable contact forces $\boldsymbol{\lambda} = \mathbf{G}_K^R\mathbf{g} + \mathbf{E}\boldsymbol{y}$. Then, a sufficient condition for having a contact force perturbation $\Delta\boldsymbol{\lambda}$ such that the friction constraints and the maximum force constraint are satisfied is: $\| \Delta\boldsymbol{\lambda} \| \leq d_{\min}^{\mathcal{F}_h}$. If we evaluate the external wrench disturbance that satisfies these constraints we get

$$\| \Delta\mathbf{g} \| \leq \frac{d_{\min}^{\mathcal{F}_h}}{\sigma_{\max}(\mathbf{G}_K^R)} \tag{6}$$

where $\sigma_{\max}$ indicates the maximum singular value.

The derivation of Eq. (6) is omitted for the sake of brevity, and can be found in [16]. The right side of Eq. (6) measures the maximum external disturbance that the grasp can resist without violating contact and friction constraints, and thus can be considered a measure of force closure property for the grasp. Since $d_{\min}^{\mathcal{F}_h}$ depends on $\boldsymbol{y}$, we can find the optimal contact force distribution $\hat{\boldsymbol{\lambda}}$ as: $\hat{\boldsymbol{\lambda}} = \mathbf{G}_K^R\mathbf{g} + \mathbf{E}\hat{\boldsymbol{y}}$, with $\hat{\boldsymbol{y}} = \operatorname{argmax}\left(d_{\min}^{\mathcal{F}_h}/\sigma_{\max}(\mathbf{G}_K^R)\right)$.

Definition 1 (Potential Contact Robustness, PCR): The value of the grasp quality corresponding to $\hat{\boldsymbol{y}}$ is called Potential Contact Robustness (PCR) and is defined in Eq. (7).

$$\mathrm{PCR} = \max_{\boldsymbol{y}} \frac{d_{\min}^{\mathcal{F}_h}}{\sigma_{\max}(G_K^R)}. \tag{7}$$

■

The PCR definition assumes that friction constraints must be satisfied for all the contact points. When a contact force does not satisfy the constraints in Eq. (4) and Eq. (5), we can have two possibilities:

1) if $\lambda_{i,n} < 0$ for some i, the i-th contact is lost, in this case we assume $\Delta\boldsymbol{\lambda}_i = 0$;
2) if $\sqrt{\lambda_{i,t}^2 + \lambda_{i,o}^2} > \mu_i \lambda_{i,n}$, the friction constraint at contact i is not satisfied, so the contact cannot apply the required tangential force. A contact force variation then has to decrease or at least maintain constant the ratio between the tangential and normal component of the contact force. A conservative hypothesis in this case is that the contact force variation that can be applied is normal to the contact surface, i.e. $\Delta\boldsymbol{\lambda}_i = \Delta\lambda_{i,n}\mathbf{n}_i$.

Let us suppose that, for a certain $\bar{\mathbf{y}}$, the first condition is verified for n_{nc} of the n_c contact points, and the second is verified for n_n contact points, then surely $n_{\text{nc}} + n_n \leq n_c$. Assume that in $n_g = n_c - n_{\text{nc}} - n_n$ the friction constraints are satisfied. Based on the previous considerations, we can define a contact force vector $\bar{\boldsymbol{\lambda}} \in \mathbb{R}^{3n_g + n_n}$ and write the object equilibrium as $\mathbf{g} + \bar{\mathbf{G}}\bar{\boldsymbol{\lambda}} = \mathbf{0}$, where $\bar{\mathbf{G}} \in \mathbb{R}^{6\times(3n_g+n_n)}$.

If the system can be still inverted, i.e. if we can still find a set of contact forces that can balance the external wrench $\mathbf{g}$ and if such forces satisfy friction constraints, the grasp is stable even if some contacts are lost and in some of the contacts the friction constraints are not satisfied. This is why the Potential Grasp Robustness (PGR), that is a generalization of the PCR, is based on the assumption that after the action of an external disturbance $\Delta\mathbf{g}$, the i-th contact can be in three different states:

- *State 1:* both constraints in (4) and (5) are satisfied at the i-th contact. In this case the contact force can be transmitted in any direction through the contact point and the contact stiffness matrix is defined as $\mathbf{K}_{\text{ic}} = diag(K_{\text{itx}}, K_{\text{ity}}, K_{\text{itn}})$, where K_{itx} and K_{ity} characterize the tangential stiffness, and K_{in} is the normal stiffness.
- *State 2:* only (4) is satisfied. In this case the contact force can be transmitted only in the normal direction to the contact: $\mathbf{K}_{\text{ic}} = K_{\text{itn}}$.
- *State 3:* both constraints in (4) and (5) are violated. In this case the contact is considered as detached, so the contact stiffness is the empty matrix: $\mathbf{K}_{\text{ic}} = []$.

Given a certain grasp, the state of each contact is *a priori* unknown, thus with n_c contact points, there are 3^{n_c} possible configurations C_j of contact states and each of them will have a certain global stiffness matrix $\mathbf{K}(C_j) = (\mathbf{K}_c^{-1} + \mathbf{J}\mathbf{K}_q^{-1}\mathbf{J}^T)^{-1}$, where $\mathbf{K}_c = diag(\mathbf{K}_{1c}, \ldots, \mathbf{K}_{n_c c})$. Note that, according to the definitions above, for the computation of the PCR index, we consider just one grasp configuration in which all contacts are in State 1.

Definition 2 (Potential Grasp Robustness, PGR): Let us define the quantity $d_{\min}^{\mathcal{F}_h}(C_j)$ as the minimum element of the vector $\mathbf{d}(\boldsymbol{\lambda})$ with $\boldsymbol{\lambda} = \mathbf{G}_{K(C_j)}^R \mathbf{g} + \mathbf{E}(C_j)\boldsymbol{y}$. The Potential Grasp Robustness (PGR), is then defined as:

$$\text{PGR} = \max_{\text{C}_\text{j}} \max_{\boldsymbol{y}} \frac{d_{\min}^{\mathcal{F}_h}(C_j)}{\sigma_{\max}(\mathbf{G}_{\mathbf{K}(C_j)}^R)} \tag{8}$$

$$\text{subject to} \quad \mathcal{N}(\mathbf{K}(C_j)\mathbf{G}^T) = \mathbf{0} \tag{9}$$

and it maximizes the distance from the violation of the constraints over the vectors $\boldsymbol{y}$, and over the configurations C_j. Condition (9) must be satisfied to immobilize the object [1]. Note that both, the pseudoinverse of $\mathbf{G}$, $\mathbf{G}_{\mathbf{K}(C_j)}^R$, and the basis of controllable internal forces, $\mathbf{E}(C_j)$, depend on the configuration C_j. ■

TABLE I
COEFFICIENTS OF THE CONSTRAINTS IN EQ. (11).

Constraint type	$\alpha_{i,k}$	$\gamma_{i,k}$	$\delta_{i,k}$
Friction cone ($k = f$)	α_i	-1	0
Min. normal force ($k = m$)	0	-1	$f_{i,\min}$
Max. force module ($k = M$)	1	0	$-f_{i,\max}$

B. Algorithm

The definition of the PGR given in Eq. (8) is based on geometrical considerations and is rather intuitive. To improve the numerical efficiency of the optimization problem in (8), and to avoid convergence problems that may arise and that we experienced in some preliminary simulations, we chose to follow the method explained in [15], where the grasp quality is computed with an algorithm that, similarly to [16], measures of how far are the contact forces from violating the friction constraints, and that, under suitable hypotheses, has a global solution.

The algorithm introduced in [15] is an efficient way to determine whether a grasp has force closure or not for SPwF contacts, and it is based on the minimization of a cost function $V(\mathbf{y})$ that accounts for the friction constraints and the limitations on the magnitude of the contact forces. The solution of the optimization problem is the vector $\hat{\mathbf{y}}$ such that:

$$\hat{\mathbf{y}} = \arg\min(V(\mathbf{y})), \tag{10}$$

For the sake of clarity, we summarize here the evaluation of $V(\mathbf{y})$. The Coulomb friction constraint, defined in Eq. (5), can be rewritten as $\sigma_{i,f} = \alpha_i \parallel \boldsymbol{\lambda}_i \parallel - \boldsymbol{\lambda}_{i,n} < 0$, where $\alpha_i = (\sqrt{1+\mu_i^2})^{-1}$. Then we can impose a lower bound to the magnitude of the normal component of the contact force, and an upper bound to the total magnitude of the contact force: $\sigma_{i,m} = f_{i,\min} - \boldsymbol{\lambda}_{i,n} < 0$ and $\sigma_{i,M} = \parallel \boldsymbol{\lambda}_i \parallel - f_{i,\max} < 0$.

The three constraints listed above can be expressed with a single inequality as in Eq. (11), where $i = 1, \cdots, n_c$ indicates the contact point, $k = f, m, M$ indicates the constraint type, and $\alpha_{i,k}$, $\gamma_{i,k}$, and $\delta_{i,k}$ are constant parameters defined in Table I.

$$\sigma_{i,k} = \alpha_{i,k} \parallel \boldsymbol{\lambda}_i \parallel + \gamma_{i,k}\boldsymbol{\lambda}_{i,n} + \delta_{i,k} < 0 \tag{11}$$

Let us define $\Omega_{i,k}^{\epsilon} \subset \mathbb{R}^h$ the set of vectors $\mathbf{y}$ that, for a given external wrench $\mathbf{g}$, satisfy the constraint in Eq. (11) with a certain margin ϵ: $\Omega_{i,k}^{\epsilon} = \{\mathbf{y} | \sigma_{i,k}(\mathbf{g}, \mathbf{y}) < -\epsilon\}$.

Then we can define, for each contact i and each constraint k, the following functions:

$$V_{i,k}^{\epsilon}(\mathbf{g}, \mathbf{y}) = \begin{cases} (d\sigma_{i,k}^2)^{-1} & \mathbf{y} \in \Omega_{i,k}^{\epsilon} \\ a\sigma_{i,k}^2 + b\sigma_{i,k} + c & \mathbf{y} \notin \Omega_{i,k}^{\epsilon} \end{cases}.$$

The function $V(\mathbf{g}, \mathbf{y})$ is then evaluated as $V(\mathbf{g}, \mathbf{y}) = \sum_{i=1}^{n_c} \sum_{k=f,m,M} V_{i,k}^{\epsilon}(\mathbf{g}, \mathbf{y})$.

In [15] and [19] it has been shown that, by properly choosing the coefficients a, b, c, and d, the function $V_{i,k}^{\epsilon}(\mathbf{g}, \mathbf{y})$ is twice continuously differentiable, and that $V(\mathbf{g}, \mathbf{y})$ is strictly convex. These two conditions ensure that the solution to the minimization problem (10) is global, provided that it exists.

We can say that V measures the distance of the grasp from violating the constraints listed before: the smaller is V, the larger is the distance. For this reason, after having found the solution $\hat{\mathbf{y}}$, we can use the reciprocal of $V(\hat{\mathbf{y}})$ as a measure of the quality of the grasp. In particular, we propose in this paper an alternative measure of PCR (Eq. (12)).

$$\text{PCR} = \frac{1}{V(\hat{\boldsymbol{y}})} \tag{12}$$

We can observe that if just one of the constraints is not satisfied or if it is near to its boundary, $V_{i,k}(\mathbf{g}, \mathbf{y})$ quickly increases and therefore the PCR becomes very small. As previously observed, a stable equilibrium configuration can be found also if friction constraints are not satisfied for all the contact points. The PGR considers this possibility and provides a less conservative measure of grasp quality. In this paper we propose, for the evaluation of the PGR, the following expression:

$$\text{PGR} = \max_{C_j} \frac{1}{V(\hat{\boldsymbol{y}}, C_j)} = \max_{C_j} \text{PCR}(C_j) \tag{13}$$

$$\text{subject to} \qquad \mathcal{N}(\mathbf{K}(C_j)\mathbf{G}^T) = \mathbf{0} \tag{14}$$

The computation of the PGR is summarized in Alg. 1.

Remark 1 (Considerations about PCR and PGR): Both PCR and PGR consider the main grasp properties: contact points, contact normals, friction coefficient, etc., but also hand degrees of freedom (DoFs) and consequently the directions of controllable contact forces. This is why these quality indexes can be applied to underactuated and compliant hands.

We have seen that the PCR and PGR indexes search for the optimal contact force distribution, based on different assumptions. The PCR is very conservative, because it relies on the assumption in Eq. (2), thus considering that the forces are univocally determined by the kinematic of the grasp. The PGR, instead, is based on the hypothesis that not all the contacts are necessary to guarantee grasp stability, and that the contact force variation at a generic contact can be either zero, if the contact point is detached, normal to the contact surface, if the variation predicted by the quasi-static model approaches the boundary of the friction cone, or a generic three dimensional force, if both contact and friction constraints are verified. We acknowledge that this solution is an approximation of the actual distribution of the contact forces, that could be evaluated only with a dynamical simulation including a nonlinear friction model. However, this approach leads to a feasible solution, that complies with both, equilibrium equations and friction constraints, and is less conservative than the one proposed in [15], even if probably more conservative than the actual distribution.

The main idea of our approach is that, if we find a feasible stable solution that satisfies all system constraints, this means that an equilibrium configuration exists and can be stably reached. The actual new equilibrium configuration may be different from the one predicted by the evaluation that we propose, but not worse. A worse solution, in terms of grasp quality, would mean higher tangential forces, unnecessary for system equilibrium, leading to higher stress distributions and therefore higher strain energy. Such a solution then would contradict the Principle of Least Work [20]. If we can find a stable equilibrium solution, it may be different from the actual one, but for sure, in terms of grasp robustness, it will be more conservative. ■

Algorithm 1: Computation of the Potential Grasp Robustness.

```
Each contact point can be in one of these three states:
   attached (State 1), sliding (State 2), detached (State 3).
Find the combinations C_1, C_2, ..., C_{3^{n_c}} of the 3 states
   for the n_c contact points.
for j = 1 : 3^{n_c}
      compute the PCR for combination C_j: PCR(C_j)
PGR = max_{C_j} PCR(C_j)
```

IV. Numerical Simulations

Here some examples of PCR and PGR evaluation are presented. The indexes were computed using SynGrasp MATLAB Toolbox [21] for two different grasp configurations. In the first one we considered a single arm, modeled with 4 joints. In the second one we considered an anthropomorphic hand, with 5 fingers and 20 DoFs. In both the examples, we considered a synergy actuation system [22], to investigate the changes in the grasp quality depending on the number of activated actuators. For the single arm we artificially chose the synergy matrix reported in (15), whereas for the anthropomorphic hand we used the synergy matrix defined by Santello *et al.* [23].

$$S = \begin{bmatrix} 1 & 1 & 1 & 1 \\ 1 & 1 & 1 & 0 \\ 1 & 1 & 0 & 0 \\ 1 & 0 & 1 & 0 \end{bmatrix} \tag{15}$$

For the sake of simplicity, in simulations we assume that all contact points have the same force limits and friction coefficient: $f_{i,\min} = f_{\min}$, $f_{i,\max} = f_{\max}$, and $\mu_i = \mu$, $\forall i \in \{1, \ldots, n_c\}$. Since PCR and PGR depend on the hand actuation and also on μ, $f_{\min}$ and $f_{\max}$, we decided to evaluate the indexes with respect to these parameters, similarly to [24]. For the sake of brevity we will only show results obtained when varying μ (Fig. 2); results obtained when varying $f_{\min}$ and $f_{\max}$ are analogous.

This section has three subsections. In Section IV-A we report the results obtained when computing the PGR according to Eq. (13), in Section IV-B we introduce heuristics to compute the PGR for power grasps in a new and efficient way, and in Section IV-C we briefly present the comparison between the PGR and a classical grasp quality measure.

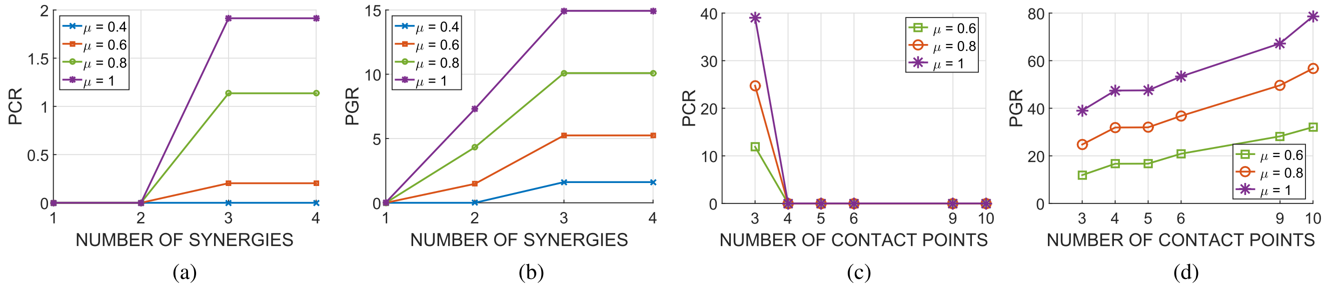

Fig. 2. (a), (b) PCR and PGR for a single arm grasping an object in 4 contacts with respect to the number of actuated synergies and the friction coefficient μ. (c), (d): PCR and PGR for the anthropomorphic hand with 3 actuated synergies with respect to n_c and μ.

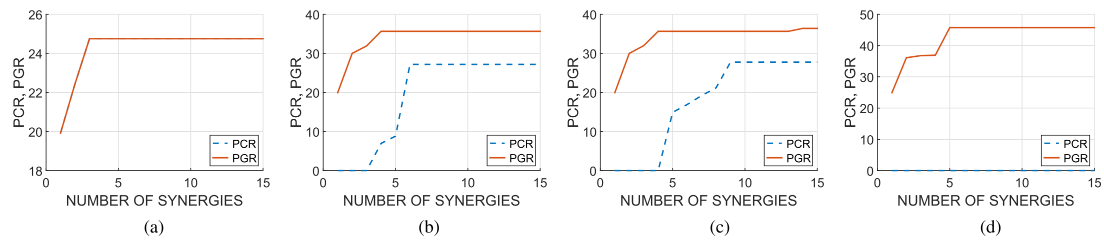

Fig. 3. PCR and PGR computed for the anthropomorphic hand. (a) $n_c = 3$. (b) $n_c = 4$. (c) $n_c = 5$. (d) $n_c = 6$

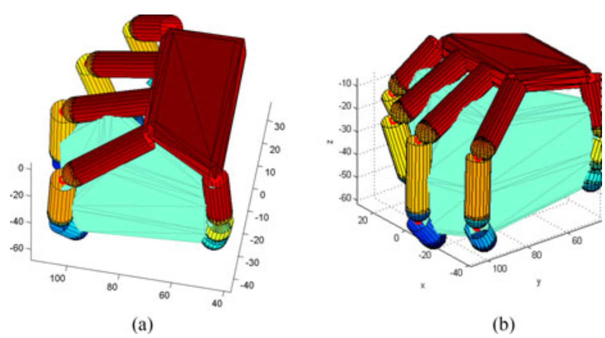

Fig. 4. Simulated power grasps with $n_c = 9$ and $n_c = 15$.

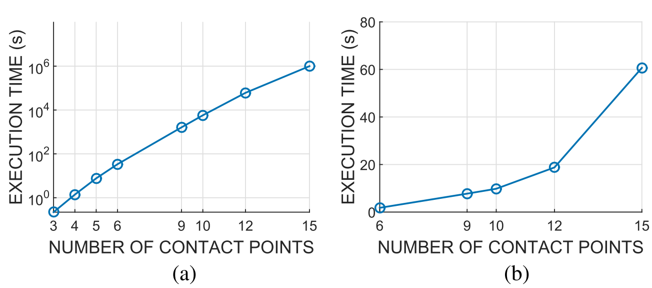

Fig. 5. Computation time of the PGR obtained (a) following its definition, and (b) with Heuristic 2 with $h = 3$.

A. PGR Computed Without Heuristics

Fig. 2(a) and (b) show the values of PCR and PGR obtained when varying the friction coefficient μ and the number of actuated degrees of freedom (x-axis) for a power grasp with the single arm. The remarkable characteristics of the graphs are mainly three: i) the quality of the grasp increases when the constraint is relaxed, i.e. for greater values of μ; ii) for $n_c \geq 2$ the PGR is always grater than the PCR, due to its definition; iii) the PGR detects that a stable grasp is possible also with two actuated degrees of freedom, while the PCR does not provide such an information (PCR $\approx 10^{-10}$).

Fig. 3 shows how PCR and PGR vary for the anthropomorphic hand with respect to the number of activated synergies in fingertip grasps with 3, 4, and 5 contacts, and in a grasp with 6 contacts located in the fingertips and middle phalanges of the thumb, index, and middle finger. The results for precision grasps confirm that both indexes depend on the degree of actuation of the hand, since they are non-decreasing with respect to the number of activated synergies. Fig. 3(d) shows that the PCR cannot detect that the grasp is robust (PCR $\approx 10^{-11}$), while the PGR, not only is greater than the PCR, but also, given a certain actuation, it is larger than in the other cases (Fig. 3(a)–(c)). In Fig. 2(c) and (d) we report how the quality measures computed for the anthropomorphic hand with three activated synergies, vary with respect to n_c and μ. We chose this type of actuation because neuroscientific studies showed that the majority of human grasps is a combination of the first three synergies [23]. Note that the contact points in the grasp with $n_c = 9$ (Fig. 4(a)) are placed like in the one with $n_c = 6$, but include also the proximal phalanges of the first three fingers, while in the grasp with $n_c = 10$, each of the 5 fingers has one contact on the fingertip and one on the proximal phalanx. Fig. 2(d) shows that the PGR i) finds stable grasp configurations also with few activated synergies, ii) grows with n_c, and iii) grows with the value of μ. The PCR, instead, is very close to zero ($\approx 10^{-12}$) for $n_c \geq 4$. The different behaviors of the two quality measures are due to their definitions (Eq. (7), (8)): the PGR is less conservative than the PCR and searches for the best grasp over a bigger configuration space.

B. PGR Computed With Heuristics

As discussed in Section III, the number of possible combinations C_j is exponential in n_c and thus, computing the PGR

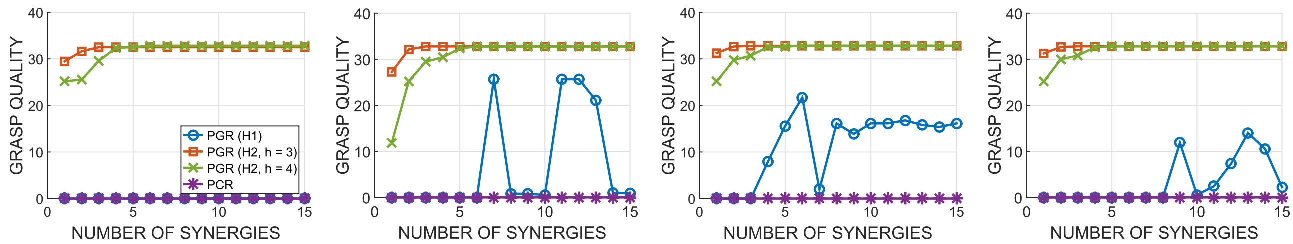

(a) (b) (c) (d)

Fig. 6. PGR computed in three different ways and PCR for four power grasps of the anthropomorphic hand. (a) $n_c = 9$. (b) $n_c = 10$. (c) $n_c = 12$. (d) $n_c = 15$

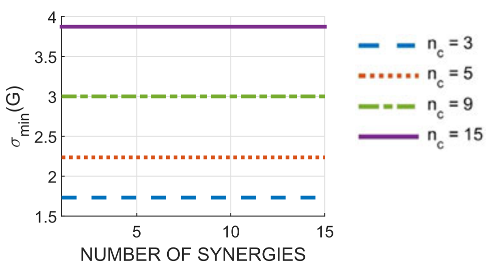

Fig. 7. Minimum singular value of $\mathbf{G}$ evaluated with respect to n_c and n_z.

Algorithm 2: Heuristic 1.

1: Preload of contact forces $\boldsymbol{\lambda}_0$.
2: Evaluation of the friction constraints in each contact.
3: The contacts in which the contact force is out or too close to the friction cone, are fixed in State 2. Thus, the possible grasp configurations are: $C_1, \ldots, C_{3^{(n_c - n_n)}}$.
4: The PGR is computed as in Eq. (13).

Algorithm 3: Heuristic 2.

1: Choose h such that $3 \le h < n_c$
2: Each contact point can be either attached or detached
3: Find the combinations of contacts $C_1, C_2, \ldots, C_{\binom{n_c}{h}}$ such that in each combination there are h attached contacts and $n_c - h$ detached contacts.
4: The PGR is computed as in Eq. (13).

for enveloping grasps, leads to very high computation times (Fig. 5(a)). This is why we decided to find heuristics to compute the PGR in a faster way, while maintaining its advantages. Alg. 2 and Alg. 3 summarize the implementation of two of them: Heuristic 1 (H1) and Heuristic 2 (H2).

In this section we will use PGR_{woH}, PGR_{H1}, and PGR_{H2} to indicate the PGR computed without heuristics, with H1, and with H2, respectively.

Heuristic 1 is articulated in three main steps. The initial contact forces (preload) are computed as: $\boldsymbol{\lambda}_0 = \mathbf{E}\hat{\boldsymbol{y}}$, where $\mathbf{E}$ is a basis for the subspace of the controllable internal forces and $\hat{\boldsymbol{y}}$ is the same of Eq. (10). Then, the distance of $\boldsymbol{\lambda}_{0,i}$ from the i-th contact cone is evaluated as: $\phi - \beta_i$, where ϕ is the amplitude of the friction cone ($\phi = \arctan(\mu)$) and β_i is the angle between $\boldsymbol{\lambda}_{0,i}$ and the normal to the contact. If $\phi - \beta_i < \eta$, where η is a positive, empirically chosen, threshold equal to 1°, then the contact is fixed in State 2 because it is out of the friction cone or too close to it. Assuming that n_n contacts are fixed in State 2, only $3^{(n_c - n_n)}$ grasp configurations will be taken into account during the computation of the grasp quality. This is why in some cases (Fig. 6), $\mathrm{PGR}_{H1} \approx 0$, like the PCR. However, from our simulations, we found that H1 presents the following advantages: $i)$ for some actuation configurations it finds a better result than the PCR, $ii)$ it has a lower computation time than H2. In future developments of this study we will further consider this heuristic, and in particular the role of the threshold η. On the basis of some preliminary tests, we expect that for higher values of this parameter, H1 will give more realistic results in terms of quality measure, but will require a longer computation time.

To implement the second heuristic, summarized in Alg. 3, we started from the consideration that a force closure grasp in $3D$ space can be achieved with at least three SPwF contact points [1]. The first step of Alg. 3 is the assumption that the hand can transmit force at only h out of n_c contact points, with $h \ge 3$. Then, the PGR is computed considering only the combinations C_j with h attached contact points and $n_c - h$ detached contact points. H2 allows us to understand which are the contact points that stabilize the grasp, in which it is worth applying a force. Fig. 5(b) shows the computation times of H2, and Fig. 6 presents the results obtained when applying the heuristics to three different power grasps. Those with $n_c = 9$ and $n_c = 10$ are the same of Section IV-A, the one with $n_c = 15$ (Fig. 4(b)) has three contacts (fingertip, middle phalanx, proximal phalanx) per finger, and the one with $n_c = 12$ is like the case with 15 contacts, but without the little finger.

Time values in Fig. 5 were obtained on a Intel Core i7-5500U with a 16GB RAM, and the algorithm was implemented in MATLAB 2015a. Note that the value reported in Fig. 5(a) for $n_c = 15$ is actually only an estimate based on the knowledge of the computation times obtained in the other cases.

In Fig. 6 H2 is computed for $h = 3$ and $h = 4$. The interesting result is that the grasp quality does not change significantly in the two cases, suggesting that three contacts are sufficient for establishing a robust grasp. From Fig. 6 we can also argue that $i)$ the PCR index fails to detect enveloping grasps, and $ii)$ H2 predicts much better than H1 the robustness of the grasp, because it increases with the number of activated synergies and agrees with the intuition that grasps with 9, 10, 12, and 15 contact points are stable. Let us now compare the PGR values computed with H2 with $h = 3$, with those obtained without heuristics. The data relative to the anthropomorphic hand with 3 activated synergies and $n_c = 9, 10, 12$ are, respectively: $\mathrm{PGR}_{H2} = [32.50, 32.78, 32.80]$, and $\mathrm{PGR}_{woH} = [49.65, 56.72, 64.64]$. It is important to notice that PGR_{H2} grows with n_c like PGR_{woH}, but in a slower way, due to the fact that H2 considers only 3 attached contacts.

C. PGR Compared to a Classical Quality Measure

Since each grasp quality measure in the literature takes into account different aspects of a grasp [11], we can only compare PCR and PGR with other indexes in terms of general behavior and not in terms of values.

Here we describe how one of the simplest classical measures, namely the Minimum Singular Value of the Grasp Matrix ($\sigma_{\min}(\mathbf{G})$) [11], varies with respect to the number of contact points n_c and with respect to the number of activated synergies n_z. Note that the larger is $\sigma_{\min}(\mathbf{G})$, the better is the grasp. Fig. 7 shows that the grasp quality increases with n_c, but does not vary with respect to the hand actuation. This happens because $\sigma_{\min}(\mathbf{G})$ is a purely geometrical measure, based only on the position of the contact points on the object. This behavior is common to all the measures that do not take into account the hand actuation and structure.

V. Conclusion and Future Works

This work is a first step towards new and effective quality measures for power grasps with underactuated and compliant hands. In particular, the Potential Grasp Robustness index is analyzed and computed for various types of grasps. Simulations show that it is a more realistic and less conservative quality measure then the Potential Contact Robustness, and has many desirable properties: it increases with the number of contact points and the degree of actuation of the hand, and it considers friction and contact force limits.

However, the PGR has an important drawback: the time needed to compute it is very high. This is due to the fact that the number of possible combinations that must be evaluated is exponential in the number of contacts (3^{n_c}). To overcome this issue, we implemented two main heuristics and we found out that using them reduces the computation time by three orders of magnitude. Heuristic 2 presents the best trade-off between efficiency and accuracy in the evaluation of the grasp quality. Lower simulation times could also be achieved, for example, using a compiled version of the algorithms, but still the high computational cost makes the PGR in the current implementation unsuitable for grasp planner procedures. Future work will focus on accelerating the computation of the indexes using advanced optimization techniques, such as combinatorial optimization.

Another interesting aspect that we will address, is evaluating the Potential Grasp Robustness for real grasps with human hands and underactuated and compliant robotic hands. Since PGR is based on the knowledge of contact points and contact forces, the sensory system of the hand will be in this case a fundamental aspect to be considered.

References

[1] D. Prattichizzo and J. C. Trinkle, "Grasping," in *Springer Handbook of Robotics*, B. Siciliano and O. Khatib, Eds. New York, NY, USA: Springer, 2016, pp. 955–988.

[2] F. Sanfilippo, H. Zhang, K. Y. Pettersen, G. Salvietti, and D. Prattichizzo, "Modgrasp: an open-source rapid-prototyping framework for designing low-cost sensorised modular hands," in *Proc. IEEE-RAS Int. Conf. Biomed. Robot. Biomechatronics*, 2014, pp. 951–957.

[3] J. Butterfass, M. Grebenstein, H. Liu, and G. Hirzinger, "DLR-hand II: next generation of a dextrous robot hand," in *Proc. IEEE Int. Conf. Robot. Autom.*, 2001, vol. 1, pp. 109–114.

[4] A. M. Dollar and R. D. Howe, "Joint coupling design of underactuated grippers," in *Proc. 30th Annu. Mech. Robot. Conf.*, 2006, pp. 903–911.

[5] C. D. Santina, G. Grioli, M. Catalano, A. Brando, and A. Bicchi, "Dexterity augmentation on a synergistic hand: The pisa/iit softhand+," in *Proc. IEEE-RAS Int. Conf. Humanoid Robot.*, 2015, pp. 497–503.

[6] R. Deimel and O. Brock, "A novel type of compliant and underactuated robotic hand for dexterous grasping," *Int. J. Robot. Res.*, vol. 35, no. 1–3, pp. 161–185, Jan. 2016.

[7] S. Krut, V. Bégoc, E. Dombre, and F. Pierrot, "Extension of the form closure property to underactuated hands," *IEEE Trans. Robot.*, vol. 26, no. 5, pp. 853–866, Oct. 2010.

[8] L. U. Odhner and A. M. Dollar, "Dexterous manipulation with underactuated robotic hands," in *Proc. IEEE Int. Conf. Robot. Autom.*, Shanghai. China, 2011, pp. 5254–5260.

[9] S. Krut, "A force-isotropic underactuated finger," in *Proc. IEEE Int. Conf. Robot. Autom.*, Barcelona, Spain, 2005, pp. 2314–2319.

[10] C. Ferrari and J. Canny, "Planning optimal grasps," in *Proc. IEEE Int. Conf. Robot. Autom.*, 1992, pp. 2290–2295.

[11] M. A. Roa and R. Suarez, "Grasp quality measures: review and performance," *Auton. Robot.*, vol. 38, no. 1, pp. 65–88, 2015.

[12] N. Pollard, "Closure and quality equivalence for efficient synthesis of grasps from examples," *Int. J. Robot. Res.*, vol. 23, no. 6, pp. 595–614, 2004.

[13] T. Omata and K. Nagata, "Rigid body analysis of the indeterminate grasp force in power grasps," *IEEE Trans. Robot. Autom.*, vol. 16, no. 1, pp. 46–54, Feb. 2000.

[14] A. Bicchi, "Force distribution in multiple whole-limb manipulation," in *Proc. IEEE Int. Conf. Robot. Autom.*, Atlanta, 1993, pp. 196–201.

[15] A. Bicchi, "On the closure properties of robotic grasping," *Int. J. Robot. Res.*, vol. 14, no. 4, pp. 319–334, 1995.

[16] D. Prattichizzo, J. K. Salisbury, and A. Bicchi, "Contact and grasp robustness measures: Analysis and experiments," in *Experimental Robotics-IV (ser. Lecture Notes in Control and Information Science 223)*, O. Khatib and K. Salisbury, Eds. Berlin, Germany: Springer-Verlag, 1997.

[17] D. Prattichizzo, M. Malvezzi, M. Gabiccini, and A. Bicchi, "On motion and force controllability of precision grasps with hands actuated by soft synergies," *IEEE Trans. Robot.*, vol. 29, no. 6, pp. 1440–1456, Dec. 2013.

[18] R. M. Murray, Z. Li, and S. S. Sastry, *A Mathematical Introduction to Robotic Manipulation*. Boca Raton, FL, USA: CRC, 1994.

[19] A. Bicchi and D. Prattichizzo, "Analysis and optimization of tendinous actuation for biomorphically designed robotic systems," *Robotica*, vol. 18, no. 1, pp. 23–31, 2000.

[20] O. A. Bauchau and J. I. Craig, *Structural Analysis: With Applications to Aerospace Structures*. New York, NY, USA: Springer, 2009, vol. 163.

[21] M. Malvezzi, G. Gioioso, G. Salvietti, and D. Prattichizzo, "Syngrasp: A matlab toolbox for underactuated and compliant hands," *IEEE Robot. Autom. Mag.*, vol. 22, no. 4, pp. 52–68, Dec. 2015.

[22] D. Prattichizzo, M. Malvezzi, M. Gabiccini, and A. Bicchi, "On motion and force controllability of precision grasps with hands actuated by soft synergies," *IEEE Trans. Robot.*, vol. 29, no. 6, pp. 1440–1456, Dec. 2013.

[23] M. Santello, M. Flanders, and J. F. Soechting, "Postural hand synergies for tool use," *J. Neurosci.*, vol. 18, no. 23, pp. 10 105–10 115, 1998.

[24] M. Gabiccini, A. Bicchi, D. Prattichizzo, and M. Malvezzi, "On the role of hand synergies in the optimal choice of grasping forces," *Auton. Robot.*, vol. 31, no. 2/3, pp. 235–252, 2011.